MOLECULAR AND CELLULAR BIOLOGY, July 2008, p. 4459–4468 Vol. 28, No. 14
0270-7306/08/$08.00+0 doi:10.1128/MCB.00410-08

PR-Set7 Establishes a Repressive *trans*-Tail Histone Code That Regulates Differentiation▽†

Jennifer K. Sims and Judd C. Rice*

Department of Biochemistry and Molecular Biology, University of Southern California Keck School of Medicine, Los Angeles, California 90033

Received 11 March 2008/Returned for modification 16 April 2008/Accepted 1 May 2008

Posttranslational modifications of the DNA-associated histone proteins play fundamental roles in eukaryotic transcriptional regulation. We previously discovered a novel *trans*-tail histone code involving monomethylated histone H4 lysine 20 (H4K20) and H3 lysine 9 (H3K9); however, the mechanisms that establish this code and its function in transcription were unknown. In this report, we demonstrate that H3K9 monomethylation is dependent upon the PR-Set7 H4K20 monomethyltransferase but independent of its catalytic function, indicating that PR-Set7 recruits an H3K9 monomethyltransferase to establish the *trans*-tail histone code. We determined that this histone code is involved in a transcriptional regulatory pathway in vivo whereby monomethylated H4K20 binds the L3MBTL1 repressor protein to repress specific genes, including *RUNX1*, a critical regulator of hematopoietic differentiation. The selective loss of monomethylated H4K20 at the *RUNX1* promoter resulted in the displacement of L3MBTL1 and a concomitant increase in *RUNX1* transcription. Importantly, the lack of monomethylated H4K20 in the human K562 multipotent cell line was specifically associated with spontaneous megakaryocytic differentiation, in part, by activating *RUNX1*. Our findings demonstrate that this newly described repression pathway is required for regulating proper megakaryopoiesis and suggests that it is likely to function similarly in other multipotent cell types to regulate specific differentiation pathways.

The eukaryotic genome is packaged and functionally organized into chromatin, a structure composed of DNA and chromosome-associated proteins. The most fundamental repeating unit of chromatin is the nucleosome, which consists of 146 base pairs of DNA wrapped around an octamer of the core histone proteins H2A, H2B, H3, and H4. The crystal structure of the nucleosome core particle indicates that the N-terminal tails of the histones extend from the nucleosome to interact with the nuclear environment (19). Decades' worth of research has demonstrated that specific amino acids on the histone tails are targets of various posttranslational modifications, including acetylation, phosphorylation, ubiquitination, poly(ADP) ribosylation, and methylation, and that specific modified histone residues are associated with certain biological processes (29). These observations led to the "histone code" hypothesis, where the modified histone tails, either alone or in combination, play a direct role in regulating essential DNA-templated processes, such as transcription, DNA damage and repair, recombination, and replication (37). Increasing evidence indicates that specific modified histone residues recruit and bind certain types of regulatory proteins that are involved in initiating the particular DNA-templated process (42).

Recent reports demonstrate that multiprotein complexes that modify histones and those that bind histone modifications play critical roles in developmental pathways, in part, by regulating the expression of genes involved in lineage specification (3, 20, 33). One well-defined example of this is the *Drosophila* ESC-E(Z) complex, which contains a nucleosome-specific histone methyltransferase, E(z), which specifically trimethylates histone H3 lysine 27 (H3K27) (5, 17, 23). Trimethylated H3K27 binds the chromodomain of Polycomb, a component of the PRC1 repressive complex (9, 22). This binding event and the subsequent repression of the homeotic (Hox) gene cluster represent a critical step in establishing positional identity within a developing embryo (28).

Similar to E(z), we recently codiscovered the nucleosome-specific PR-Set7 histone H4 lysine 20 (H4K20) methyltransferase, also known as Set8 or KMT5A, which is enriched within transcriptionally repressed chromatin (1, 8, 25). PR-Set7 is the only known enzyme that specifically monomethylates H4K20 in mammals; the Suv4-20 enzymes are responsible for the bulk of H4K20 di- and trimethylation (6, 35, 50). Recent structural findings demonstrated that the tandem malignant brain tumor (MBT) repeats of the L3MBTL1 repressor protein bind several mono- and dimethylated histone lysine residues in vitro (15, 18, 21). These studies also showed that L3MBTL1 preferentially binds monomethylated H4K20, a histone modification associated with repressed chromatin, strongly suggesting that they cooperate to regulate gene expression. Consistent with this, it was found that the binding of L3MBTL1 to monomethylated H4K20 creates a transcriptionally nonpermissive chromatin structure in vitro and that L3MBTL1 negatively regulates the expression of a subset of E2F target genes (44). However, unlike for Polycomb-mediated repression, the biological importance of this gene regulation pathway remains undetermined.

In this study, we extend our previous findings regarding a *trans*-tail histone code involving monomethylated H4K20 and H3K9 (36). We discovered that both modifications are dependent upon PR-Set7 and that the modifications are targeted to

* Corresponding author. Mailing address: 1450 Biggy Street, NRT 6506, Los Angeles, CA 90033. Phone: (323) 442-4332. Fax: (323) 442-7857. E-mail: juddrice@usc.edu.

† Supplemental material for this article may be found at http://mcb.asm.org/.

▽ Published ahead of print on 12 May 2008.

the same genomic regions. Importantly, the recruitment of L3MBTL1 to these regions is dependent upon PR-Set7-mediated H4K20 monomethylation and this event is required to induce gene repression. One of the genes that we discovered that is regulated by this pathway is *RUNX1*, a key regulator of hematopoietic differentiation (12). We demonstrate that the lack of monomethylated H4K20 in the human K562 multipotent cell line induces the spontaneous differentiation of these cells to megakaryocytes, in part, by activating RUNX1. Our findings indicate that this silencing pathway is required to prevent megakaryopoiesis of K562 cells and suggest that it may function similarly in other multipotent cell types to regulate differentiation.

MATERIALS AND METHODS

Plasmids and siRNA. For short hairpin RNA (shRNA), sequences specific to PR-Set7 (PR-Set7_2, 5′-CGCAACAGAATCGCAAAC; and PR-Set7_3, 5′-GAC AAATCGCCTAGGAAGA) and L3MBTL1 (5′-GGGATGATACTTA TGACTA) were cloned into the pSUPERIOR.retro.puro vector (OligoEngine). The small interfering RNA (siRNA) duplexes used include PR-Set7 (14), G9a (5′-UAAGAAUCAUCCUCUCUCAUU), L(3)MBT (5′-GUUCAGUCAUAG UAAAGAA), and lamin A/C (Dharmacon). Full-length green fluorescent protein (GFP), PR-Set7, and the R265G mutant were cloned into the pcDNA4/TO-FLAG (Invitrogen) or pCMV-Tag3A (Stratagene) vector.

Cell culture and transfections. HeLa, HEK293, and K562 cells were cultured as previously described (49). Six million HeLa cells per 10-cm plate were grown for 24 h before transfection using Lipofectamine 2000 (Invitrogen) according to the manufacturer's protocol. At 1 day posttransfection, cells were selected with 6 μg/ml puromycin for 4 days before harvesting for chromatin immunoprecipitation (ChIP), Western analysis, or quantitative reverse transcription-PCR (qRT-PCR). For siRNA, 10^5 HeLa cells were plated per well in six-well plates for transfection of RNA duplexes by use of Oligofectamine (Invitrogen) as previously described (14). Two million K562 cells were incubated with 9 μg of the indicated plasmids and 1 μg FLAG-GFP in buffer (100 mM HEPES, pH 7.4, 10 μg DEAE-dextran, Opti-MEM medium [Invitrogen]) prior to electroporation at 1,000 μF and 150 V. Cells were incubated at 37°C for 10 min before adding RPMI 1640-10% fetal bovine serum to 2 ml and equally divided into each well of a six-well plate. Forty-eight hours later, cells were pelleted, resuspended in medium with 3 μg puromycin, and grown for 5 days. Cells were washed and resuspended in RPMI 1640-10% fetal bovine serum supplemented with 0.01% dimethyl sulfoxide containing 0.1 nM, 1 nM, 10 nM, or 100 nM 12-*O*-tetradecanoylphorbol-13-acetate (TPA) for 2 days before collecting cells for fluorescence-activated cell sorting (FACS) and Western analysis.

Western analysis. Western analysis was performed as previously described (36), using the following antibodies and dilutions: H4K20 methyl-specific antibodies (LP Bio) (36), H3K9 methyl-specific antibodies (Millipore) (31), H4 general (1:60,000; Abcam), FLAG M2 (1:2,500; Sigma), H3 general (1:500,000; Abcam), RUNX1 (1:500; Abcam), G9a (1:1,000; Millipore), PR-Set7 (1:1,000) (32), and L3MBTL1 (1:1,000; LP Biologicals); horseradish peroxidase-conjugated anti-rabbit or anti-mouse antibodies (1:5,000; Jackson Immunologicals) were used prior to the addition of enhanced chemiluminescence plus reagent (GE). The results were visualized by exposure to film for 1 min.

Differentiation and sorting. K562 cells were differentiated using 10 nM TPA (Sigma) for 5 days or 50 μM hemin (Chemika) for 4 days. Megakaryocytic differentiation was analyzed by flow cytometry using anti-CD41-fluorescein isothiocyanate (eBiosciences) or anti-CD41-phycoerythrin (MoFlo; Cytomation) antibody. Erythrocyte differentiation was analyzed by benzidine staining and/or measurement of soluble hemoglobin as previously described (10, 47).

ChIPs. Cells were treated with 1% formaldehyde for 8 min before adding glycine (final concentration, 125 mM) to quench the reaction. Cells were pelleted and nuclei were extracted in NEB buffer {5 mM PIPES [piperazine-*N*,*N*′-bis(2-ethanesulfonic acid)], pH 8, 85 mM KCl, 0.5% NP-40, 1 mM phenylmethylsulfonyl fluoride, and 1 mg/ml each of aprotinin, leupeptin, and pepstatin}, pelleted, and resuspended in lysis buffer (50 mM Tris, pH 8, 10 mM EDTA, 1% sodium dodecyl sulfate) to give a final concentration of 10^8 cells/ml. Soluble chromatin was sheared to <1 kb by sonication at 4°C for 20 seconds at 40% output (Misonix) and diluted in ice-cold ChIP dilution buffer (150 mM NaCl, 16.7 mM Tris, pH 7.5, 3.3 mM EDTA, 1% Triton X-100, 0.1% sodium dodecyl sulfate, 0.5% sodium deoxycholate) to give a final concentration of 25,000 cells/μl (final volume, 200 μl) before incubation overnight at 4°C with the following antibodies: H4K20 mono- and trimethyl (4 μl and 13 μl, respectively), H3K9 monomethyl (9 μl), hemagglutinin (HA) (1 μg; Roche), myc (1 μg; Roche), H3 general (1 μg), and L3MBTL1 (20 μl). Protein A beads (GE) were incubated with the immunoprecipitated material for 1 h at 4°C, followed by a series of washes (two with ChIP dilution buffer, four with radioimmunoprecipitation assay-LiCl buffer [50 mM HEPES, 1 mM EDTA, 1% NP-40, 0.7% sodium deoxycholate, 0.5 M LiCl], and two with TE [10 mM Tris, 1 mM EDTA]), before elution of the bound DNA by use of the Chelex method as previously described (24). PCRs were performed using increasing amounts of the eluted DNA template (0.15%, 0.5%, and 1.5%) at 30 cycles for all primer sets (see Table S1 in the supplemental material).

Expression analysis. Total RNA was extracted from HeLa and K562 cells by using an RNeasy miniprep kit (Qiagen). RT reactions were performed using a reverse transcriptase kit (Applied Biosystems). Ten nanograms of the resultant cDNA was used for either semiquantitative or quantitative real-time PCRs. Quantitative PCRs were performed in quadruplicate, and change values were calculated using the $2^{-\Delta\Delta CT}$ method and plotted relative to the values for mock-treated cells, normalized to 1.

RESULTS

Monomethylation of H3K9 requires the PR-Set7 H4K20 monomethyltransferase. We previously reported that the monomethylated forms of H4K20 and H3K9 were preferentially localized to the same genomic regions in mammalian cells (36). Furthermore, we found that nucleosomes enriched in monomethylated H4K20 were also preferentially monomethylated at H3K9, strongly suggesting the existence of a *trans*-tail histone code operating at these specific loci. In addition, these findings suggested that the two histone monomethylation events are coordinately regulated, similar to previous reports regarding the trimethylated forms of H3K9 and H4K20 (35, 48). Therefore, we hypothesized that the global decrease in monomethylated H3K9 would result in a concomitant global decrease in monomethylated H4K20. To test this hypothesis, HeLa cells were transiently transfected with siRNA duplexes to specifically decrease the G9a H3K9 methyltransferase or lamin A/C as the negative control (Fig. 1A). Consistent with our previous findings (31), Western analysis indicated the selective global reductions of mono- and dimethylated H3K9 in the G9a siRNA cells compared to the levels in lamin A/C siRNA cells; no apparent changes in trimethylated H3K9 were observed. Contrary to the hypothesis, no observable global changes in the different methylated states of H4K20 were detected. Similar results were obtained using mouse embryonic fibroblasts lacking G9a (see Fig. S1 in the supplemental material) (38). These results indicate that global levels of methylated H4K20 are not dependent on G9a or global levels of mono- or dimethylated H3K9.

These findings raised the converse possibility: that monomethylated H3K9 may be dependent upon monomethylated H4K20. Since PR-Set7 is the predominant H4K20 monomethyltransferase (6, 50), we hypothesized that the depletion of monomethylated H4K20 via RNA interference for PR-Set7 would result in decreased monomethylated H3K9. Western analysis of HeLa cells transfected with two different PR-Set7 shRNA plasmids each demonstrated significant reductions of PR-Set7 and the monomethylated form of H4K20; di- and trimethylated levels were unchanged (Fig. 1B). Remarkably, the same cells displayed a near-complete global loss of monomethylated H3K9 without any detectable alterations in di- or trimethylated H3K9. To determine if these changes were dependent upon H4K20 monomethylation, cells were transfected with a catalytically dead (CD)

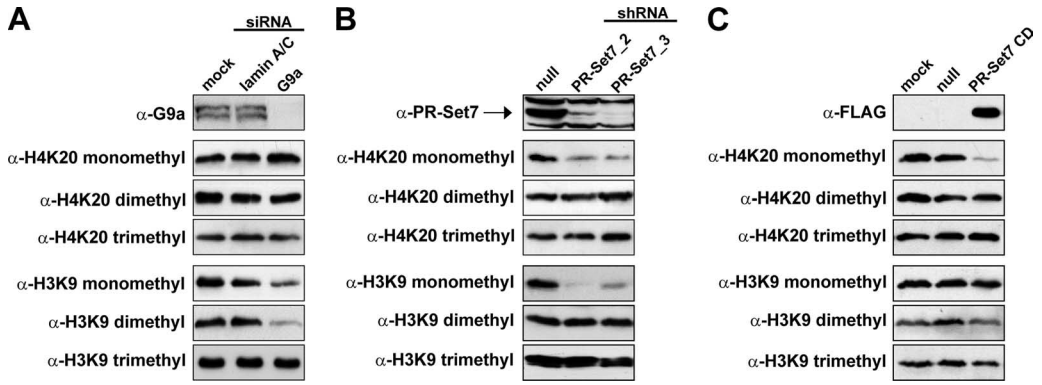

FIG. 1. H3K9 monomethylation requires PR-Set7. (A) Western analysis of HeLa whole-cell lysates treated with siRNA duplexes specific for lamin A/C or G9a to detect global changes in the different methylated states of H4K20 and H3K9. α-G9a, anti-G9a. (B) HeLa cells were transfected with two different PR-Set7-specific shRNA constructs, and Western analysis was performed to detect global changes in the methylated states of H4K20 and H3K9 compared to the levels in the empty vector (null). (C) Similar Western analysis was performed with HEK293 cells transfected with a FLAG-tagged control plasmid (null) or a dominant-negative PR-Set7 R256G CD point mutant (PR-Set7 CD) that depletes cells of monomethylated H4K20.

PR-Set7 R265G mutant that acts as a dominant negative by depleting cells of monomethylated H4K20 without reducing levels of PR-Set7 (Fig. 1C) (25). Surprisingly, Western analysis demonstrated that monomethylated H3K9 was retained in these cells despite the loss of monomethylated H4K20. These findings indicate that H3K9 monomethylation is dependent upon PR-Set7 but is independent of its catalytic function.

PR-Set7 monomethyltransferase activity is required to repress RUNX1. High-throughput genome-wide technologies were employed to identify specific genes regulated by PR-Set7 and monomethylated H4K20 (data not shown). One of the identified target genes was *AML1/RUNX1*, a master regulator of hematopoietic differentiation and a gene commonly translocated in leukemias (16). qRT-PCR was performed on the PR-Set7 shRNA and control shRNA HeLa cells to confirm these findings (Fig. 2A). As predicted, there was a >2-fold increase in *RUNX1* expression in the absence of PR-Set7 and monomethylated H4K20. *RUNX1* expression was also analyzed for HeLa cells transfected with the PR-Set7 CD plasmid to determine if the increase in expression was directly correlated with a loss of monomethylated H4K20. As we had previously observed with several other genes enriched in monomethylated H4K20 (data not shown), the absence of this histone modification resulted in a >3-fold increase in *RUNX1* expression. Concomitant with an increase in *RUNX1* mRNA levels, we also observed a significant increase in RUNX1 protein levels in the PR-Set7 shRNA cells (Fig. 2B). These findings strongly suggest that the monomethylation of H4K20 by PR-Set7 plays a key upstream regulatory role in *RUNX1* expression. Furthermore, these findings suggest that the presences of PR-Set7 protein itself and monomethylated H3K9 are not sufficient for *RUNX1* repression.

Monomethylated H4K20 and H3K9 are selectively targeted to the *RUNX1* promoter. Since we had identified that monomethylated H4K20 was enriched at the *RUNX1* promoter in HeLa cells (data not shown), we predicted that this putative silencing pathway was selectively targeted to this region to repress *RUNX1* expression. To determine this, ChIPs were performed with HeLa cells (null) by using antibodies specific for monomethylated H4K20, with a general histone H3 antibody as the positive control or preimmune rabbit IgG as the negative control. PCRs were performed for each sample by using increasing amounts of ChIP template for amplification of the *RUNX1* promoter or a region 160 kb upstream that is devoid of monomethylated H4K20 (Fig. 2C). Input DNA was used as the positive control for successful PCR amplification. Visual inspection of the PCRs verified that monomethylated H4K20 was enriched at the *RUNX1* promoter compared to that in the *RUNX1* upstream region in HeLa cells (null). Quantitative analysis was performed by first plotting the intensity of each band of a sample to determine a slope (see Fig. S2 in the supplemental material). The slope of each ChIP was then normalized to the slope of the input DNA and plotted with the standard error, generated from three independent biological replicates (Fig. 2D). Consistent with Fig. 2C, the quantitative analysis indicates an ~12-fold enrichment of monomethylated H4K20 at the *RUNX1* promoter compared to the levels in the upstream region in the HeLa cells (null). Based on the findings described above, we predicted that monomethylated H3K9 would also be specifically targeted to this region. ChIPs were performed with an H3K9 monomethyl-specific antibody, and visual inspection of the resultant PCR amplifications revealed an enrichment of monomethylated H3K9 at the *RUNX1* promoter compared to the levels in the upstream region (Fig. 2C). Quantitative analysis confirmed an ~5-fold increase of monomethylated H3K9 at the *RUNX1* promoter, providing further evidence of the selective targeting of this *trans*-tail histone code.

To further verify these findings, ChIPs were performed with HeLa cells transfected with the PR-Set7 shRNA plasmid that depletes cells of global levels of monomethylated H4K20 (Fig. 1B). Visual inspection of the PCR amplifications from the PR-Set7 shRNA cells revealed a significant reduction in monomethylated H4K20 at the *RUNX1* promoter compared to the levels in the null cells (Fig. 2C). Quantitative analysis indicated an ~10-fold decrease in monomethylated H4K20 at the *RUNX1* promoter, similar to the levels observed at the upstream region (Fig. 2D). ChIP analysis performed with the monomethyl-specific

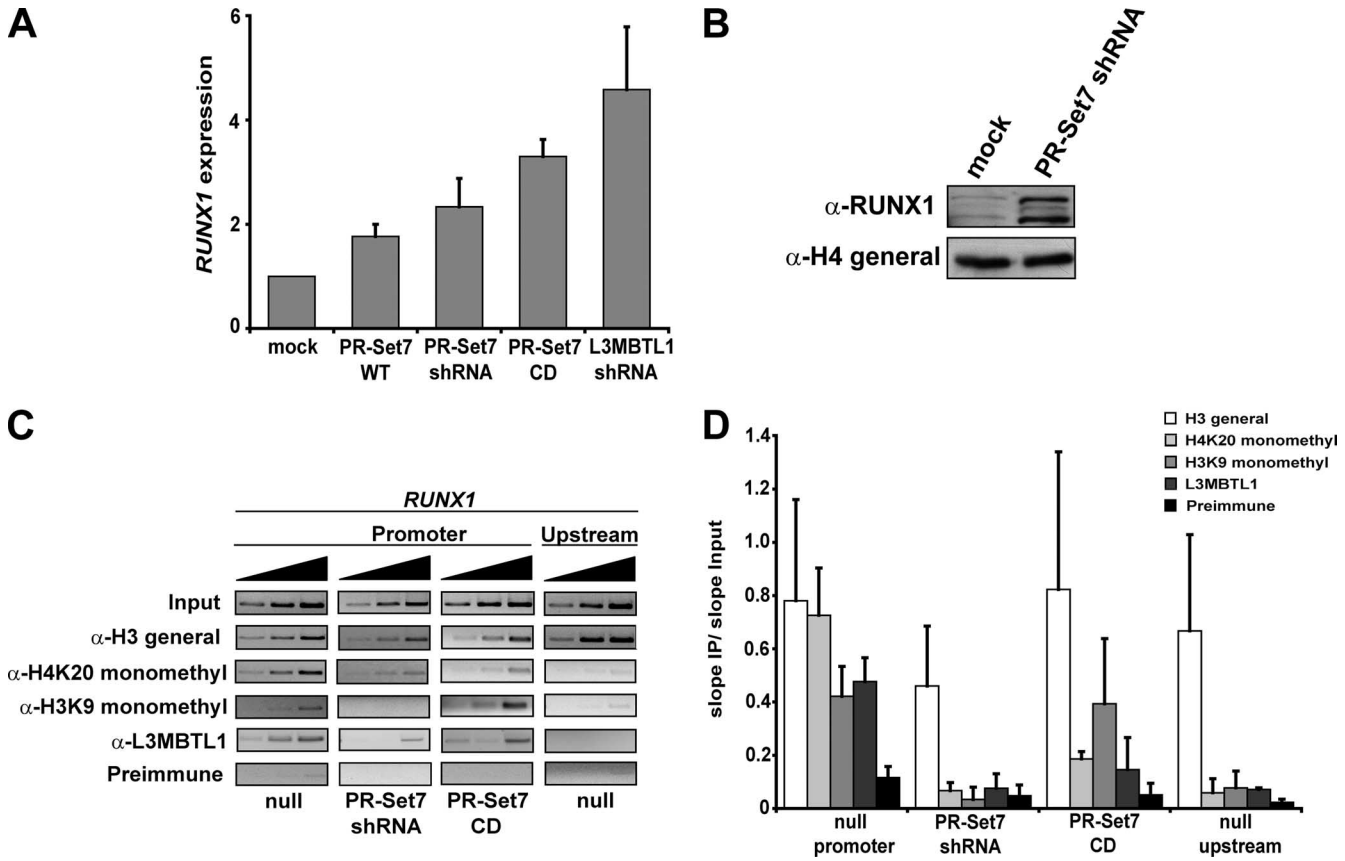

FIG. 2. Monomethylated H4K20 and L3MBTL1 at the *RUNX1* promoter is associated with *RUNX1* repression. (A) HeLa cells were transfected with a control expression vector (mock), a vector expressing full-length PR-Set7 (WT), or the R265G CD mutant or shRNA vectors that specifically deplete cells of PR-Set7 or L3MBTL1. qRT-PCR was performed to determine levels of *RUNX1* expression, normalized to those of GAPDH expression, and plotted as *n*-fold increases relative to mock levels (*y* axis). Three independent biological replicates were performed to generate standard deviations. (B) RUNX1 protein levels for the mock and PR-Set7 shRNA samples were determined by Western analysis. A general histone H4 antibody (α-H4) was used as the loading control. (C) ChIPs were performed with HeLa cells transfected with an empty vector (null), a PR-Set7 shRNA vector, or the PR-Set7 CD vector by using either an H4K20 monomethyl-specific antibody, an H3K9 monomethyl-specific antibody, an L3MBTL1 antibody, a general H3 antibody (positive control), or rabbit preimmune serum (negative control). Increasing amounts of the final ChIP-treated material (0.15%, 0.5%, and 1.5%; black triangles) were used as the template in a 30-cycle PCR amplification using primer sets specific to the *RUNX1* promoter or upstream region (negative control). Input DNA (0.005%, 0.0015%, and 0.05%) served as the positive control for PCR. (D) Semiquantitative analysis was performed by first calculating the density of each PCR band, using Quantity One (Bio-Rad). The resultant values were plotted, and the slope for each sample was determined and then graphed relative to the slope of the input (*y* axis) to reflect the degree of enrichment for each histone modification or protein. Three independent biological replicates were performed to generate standard deviations.

H3K9 antibody in the PR-Set7 shRNA cells also revealed an ~12-fold reduction of this modification at the *RUNX1* promoter compared to the levels in the null cells, similar to the levels observed at the upstream region. These findings indicate that both H4K20 and H3K9 monomethylations at the *RUNX1* promoter are dependent on PR-Set7.

Additional ChIP analysis was performed with HeLa cells transfected with the PR-Set7 CD plasmid, which serves as a dominant negative by reducing monomethylated H4K20 in the cells without decreasing PR-Set7 levels (Fig. 1C). As predicted, visualization of the PCRs demonstrates a marked reduction in monomethylated H4K20 at the *RUNX1* promoter compared to the levels in the null cells (Fig. 2C). Quantitation of the samples confirmed the reduction; however, the levels of monomethylated H4K20 at the *RUNX1* promoter were consistently higher than those in the PR-Set7 shRNA cells (Fig. 2D). This is most likely due to the inherent competition between wild-type and mutant PR-Set7 proteins in the transfected cells, resulting in the observed residual monomethylation of H4K20 at the *RUNX1* promoter. Consistent with the findings described above, ChIP analysis demonstrated no observable change in monomethylated H3K9 at the *RUNX1* promoter in the PR-Set7 CD cells compared to the levels in the null cells (Fig. 2C and D). These findings provide further evidence that both histone modifications are dependent upon the targeting of PR-Set7 to specific regions in the genome. It is also important to note that the continued presence of monomethylated H3K9 at the *RUNX1* promoter in the PR-Set7 CD cells does not inhibit *RUNX1* derepression compared to that in the PR-Set7 shRNA cells, providing further evidence that monomethylated H3K9 is not sufficient for *RUNX1* repression (Fig. 2A).

Decreased monomethylated H4K20 results in reduced L3MBTL1 at RUNX1. It was previously reported that the MBT repeats of the L3MBTL1 repressor protein selectively bind monomethylated H4K20 in vitro (15, 18, 21). Due to this as-

sociation, we theorized that L3MBTL1 was directly binding monomethylated H4K20 in vivo to repress *RUNX1* expression. Consistent with this theory, depletion of L3MBTL1 by RNA interference resulted in a >4-fold increase in *RUNX1* expression, similar to the increase observed in the absence of monomethylated H4K20, indicating a role for L3MBTL1 in regulating *RUNX1* (Fig. 2A). Based on these findings, we predicted that L3MBTL1 was targeted specifically to the *RUNX1* promoter. To test this, ChIP analysis using an L3MBTL1 antibody was performed with HeLa (null) cells. Visualization and quantitation of the PCR amplifications confirmed a significant enrichment of L3MBTL1 at the *RUNX1* promoter compared to the levels in the upstream region (Fig. 2C and D). Importantly, the depletion of PR-Set7 and monomethylated H4K20 in the PR-Set7 shRNA HeLa cells resulted in a dramatic reduction of L3MBTL1 at the *RUNX1* promoter compared to the levels in the null cells, similar to the levels observed in the upstream region. The loss of L3MBTL1 from the promoter was coincident with the derepression of *RUNX1* (Fig. 2A). ChIP analysis with the PR-Set7 CD cells revealed a marked reduction of L3MBTL1 enrichment at the *RUNX1* promoter compared to the levels in the null cells (Fig. 2C and D). However, the decreased levels of L3MBTL1 did not reach those observed in the PR-Set7 shRNA cells, most likely due to persistence of low levels of monomethylated H4K20 caused by the competition between the mutant and endogenous wild-type PR-Set7 proteins. Collectively, these findings indicate that the presence of L3MBTL1 at the *RUNX1* promoter is associated with *RUNX1* repression and that the recruitment of L3MBTL1 to this region is most likely due to its interaction with monomethylated H4K20.

Monomethylated H4K20 is required for L3MBTL1 recruitment to repress RUNX1. To verify that PR-Set7 was targeted to the *RUNX1* promoter, a myc-tagged eukaryotic expression vector encoding full-length PR-Set7 was transfected into HeLa cells for ChIP analysis using myc antibodies, since a reliable ChIP-grade PR-Set7 antibody is not yet available. While we anticipated that overexpression of the PR-Set7 monomethyltransferase would result in global increases in monomethylated H4K20, Western analysis demonstrated a significant reduction of this histone modification compared to the levels in the myc-null cells (Fig. 3A). This reduction was proportional to a dramatic global increase in trimethylated H4K20, but with no observable changes in dimethylated H4K20. ChIP analysis was performed with various antibodies at the *RUNX1* promoter in HeLa cells transfected with the myc-PR-Set7 plasmid or the myc-null control plasmid (Fig. 3B). ChIPs performed with the myc antibody demonstrated an enrichment of PR-Set7 at the *RUNX1* promoter compared to the levels in the myc-null cells, confirming that PR-Set7 is targeted to the *RUNX1* promoter (Fig. 3B). Consistent with the Western analysis, ChIPs with cells overexpressing myc-PR-Set7 demonstrated a significant reduction in monomethylated H4K20 at the *RUNX1* promoter and a concomitant increase in trimethylated H4K20. No observable changes in monomethylated H3K9 were detected at the *RUNX1* promoter. Since these cells were cotransfected with an HA-tagged eukaryotic expression plasmid encoding full-length L3MBTL1, ChIP analysis was performed using an HA antibody to assess its enrichment at the *RUNX1* promoter in these different backgrounds. The results demonstrate that

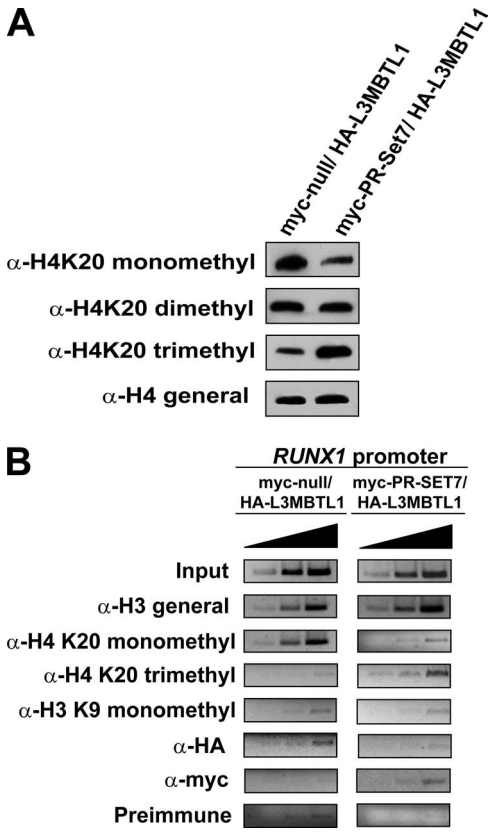

FIG. 3. Monomethylated H4K20 is required for L3MBTL1 recruitment and *RUNX1* repression. (A) HeLa cells were cotransfected with an HA-tagged L3MBTL1 plasmid and either a myc-PR-Set7 plasmid or myc-null plasmid as the negative control. Western analysis of cell lysates was performed with methyl-specific H4K20 antibodies (α-H4K20) or a general H4 antibody as the loading control. (B) ChIP analysis was performed with these cells as described for Fig. 2C.

HA-L3MBTL1 was selectively reduced in the myc-PR-Set7 cells containing decreased monomethylated H4K20 and increased trimethylated H4K20, but no change in monomethylated H3K9, at the *RUNX1* promoter compared to the levels in the myc-null cells. Importantly, the reductions of monomethylated H4K20 and L3MBTL1 at the *RUNX1* promoter in the myc-PR-Set7 cells are coincident with increased RUNX1 expression (Fig. 2A). Collectively, these findings indicate that PR-Set7 and H4K20 monomethylations are targeted to the *RUNX1* promoter and strongly suggest that *RUNX1* repression is mediated by the specific binding of L3MBTL1 to monomethylated H4K20.

Decreased monomethylated H4K20 is specifically associated with megakaryocytic differentiation. The RUNX1/AML1 transcription factor plays a critical role in mammalian hematopoiesis, in part, by regulating many hematopoietic lineage-specific genes (12). *RUNX1* expression is also tightly regulated during the establishment and maintenance of lineage-committed cells in adult megakaryopoiesis. Consistent with this, the absence of RUNX1 results in the loss of definitive hematopoiesis and is associated with defects in platelet production (13, 27). In precursor BLAST-forming unit erythroid/megakaryocte (BFU-E/MK) cells, *RUNX1* expression is repressed and remains absent

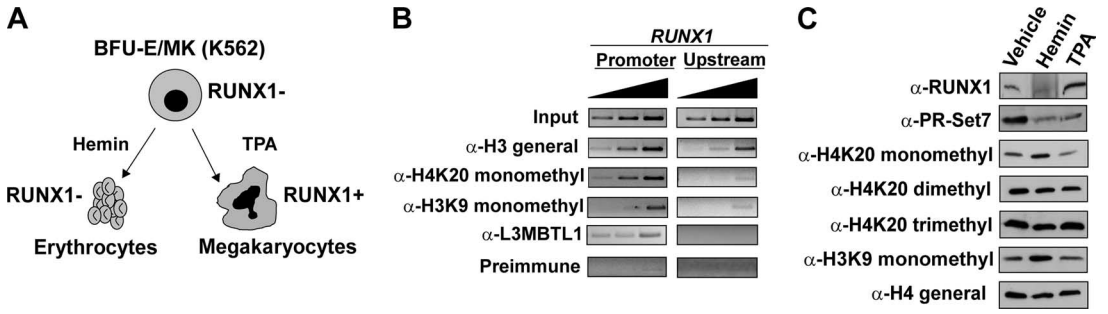

FIG. 4. Decreased monomethylated H4K20 is selectively associated with megakaryopoiesis. (A) The precursor BLAST-forming unit erythrocyte/megakaryocyte (BFU-E/MK) cells are RUNX1 negative. During erythropoiesis, the cells remain RUNX1 negative whereas RUNX1 expression is required for megakaryopoiesis. The human K562 multipotent cell line mimics BFU-E/MK cells and can be induced to selectively differentiate depending on treatment with hemin or TPA. (B) ChIP analysis was performed with K562 cells as described for Fig. 2C. α-H3, anti-H3. (C) K562 cells were treated with vehicle or either hemin or TPA to induce erythropoiesis or megakaryopoiesis, respectively. Western analysis was performed on the cell lysates by using the indicated antibodies. A general H4 antibody was used as the loading control.

during erythropoiesis (Fig. 4A) (26). In contrast, enhanced expression of *RUNX1* in precursor cells is an early event in megakaryopoiesis and recent findings demonstrate that expression of RUNX1 sensitizes precursor cells toward megakaryopoiesis (7, 13). Based on these reports and our findings described above, we predicted that PR-Set7 and monomethylated H4K20 would be reduced in cells committed to megakaryopoiesis compared to the levels in precursor cells. Since the human K562 multipotent cell line mimics precursor cells (41), we used these as the model system to determine if the components of the silencing pathway were also present at the *RUNX1* promoter. ChIP analysis revealed that, identical to the findings in HeLa cells, all components of the pathway were enriched at the *RUNX1* promoter compared to the levels in the upstream region in the wild-type K562 cells (Fig. 4B). The presence of this pathway at the *RUNX1* promoter is coincident with the repression of *RUNX1* and the absence of protein product (see Fig. S3 in the supplemental material) (7). Consistent with our data for HeLa cells, these findings indicate that monomethylated H4K20 and L3MBTL1 are associated with *RUNX1* repression in K562 cells.

The K562 multipotent cells can be chemically treated with hemin or phorbol esters to induce erythrocytic or megakaryocytic differentiation, respectively (Fig. 4A) (34, 43). Since RUNX1 is expressed specifically during megakaryopoiesis, we predicted that K562 cells treated with phorbol esters would display decreased levels of PR-Set7 and monomethylated H4K20 compared to those in vehicle-treated cells. Consistent with this hypothesis, Western analysis of K562 cells treated with the phorbol ester TPA displayed reduced levels of PR-Set7 and monomethylated H4K20 compared to those in control cells, and this was coincident with increased RUNX1 (Fig. 4C). Although we predicted a decrease in monomethylated H3K9 due to the reduction of PR-Set7, the levels remained relatively unchanged in TPA-treated K562 cells. Also unexpected was the observed decrease in PR-Set7 in K562 cells induced to the erythrocytic lineage by treatment with hemin. However, RUNX1 was not expressed in these cells, consistent with the relatively elevated global levels of both monomethylated H4K20 and H3K9. These findings strongly suggest that the specific reduction of monomethylated H4K20 is required for megakaryopoiesis in K562 cells.

Loss of monomethylated H4K20 and L3MBTL1 at the *RUNX1* promoter is an early event of megakaryopoiesis. Based on the findings described above, we predicted that the components of this new silencing pathway would be absent at the *RUNX1* promoter, specifically in the TPA-treated K562 cells, compared to the levels in vehicle control or hemin-treated cells. ChIP analysis was performed with the different heterogeneous cell backgrounds, where ~42% of hemin-treated cells were positively stained for benzidine and ~33% of the TPA-treated cells were CD41 positive (see Fig. S3 in the supplemental material). Visualization of the subsequent PCR amplifications confirmed the enrichment of monomethylated H4K20, monomethylated H3K9, and L3MBTL1 at the *RUNX1* promoter in both the vehicle control K562 cells and those treated with hemin compared to the levels in the *RUNX1* upstream region (Fig. 5A). As predicted, there were marked reductions in monomethylated H4K20 and L3MBTL1 at the *RUNX1* promoter in the TPA-treated K562 cell population. In contrast to the global analysis, there was an observable decrease in monomethylated H3K9 at the *RUNX1* promoter. Quantitation of the PCR products from three independent biological replicates, as described above, confirmed these observations (Fig. 5B). Therefore, the loss of monomethylated H4K20 and L3MBTL1 at the *RUNX1* promoter is associated with increased RUNX1 and the selective differentiation toward the megakaryocytic lineage.

Increased RUNX1 is critical during early stages of megakaryocytic differentiation as megakaryopoiesis fails to initiate without RUNX1 (13, 26). Based on our findings, we predicted that the loss of monomethylated H4K20 and L3MBTL1 from the *RUNX1* promoter was a critical upstream event required for RUNX1 activation during the commitment of precursor cells to megakaryocytes. Since expression of the CD41 cell surface marker occurs early in megakaryopoiesis, prior to increases in DNA ploidy and cell size (13), TPA-treated K562 cells in the early stages of megakaryocytic differentiation were isolated by FACS based on both their small sizes and high levels of CD41 expression. ChIP analysis was performed with these cells for comparison to K562 cells treated with vehicle. Visualization of the subsequent PCR amplifications demonstrated reductions of monomethylated H4K20 and L3MBTL1 at the *RUNX1* promoter in the early

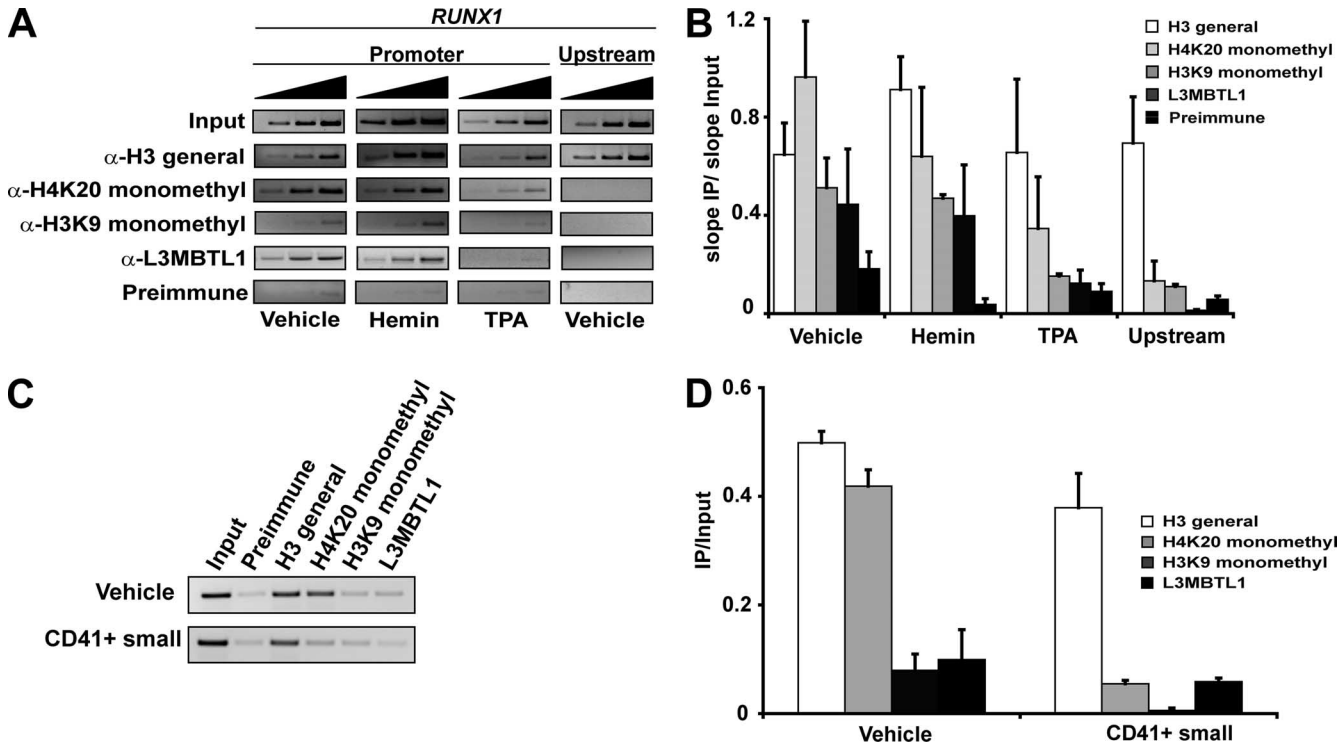

FIG. 5. Reduction of monomethylated H4K20 and L3MBTL1 at the *RUNX1* promoter is an early event in megakaryopoiesis. (A) ChIP analysis was performed with K562 cells treated with vehicle, hemin, or TPA as described for Fig. 2C. α-H3, anti-H3. (B) Semiquantitative analysis of the ChIP data was performed as described for Fig. 2D. (C) TPA-treated K562 cells in the early stages of megakaryopoiesis were isolated by FACS based on small cell size and expression of the CD41 cell surface marker. ChIP analysis was performed on these cells or vehicle-treated cells by using either an H4K20 monomethyl-specific antibody, an H3K9 monomethyl-specific antibody, a L3MBTL1 antibody, a general H3 antibody (positive control), or rabbit preimmune serum (negative control). Thirty cycles of PCR amplifications were performed using primers for the *RUNX1* promoter and 1.5% of the ChIP-treated material as the template. Input DNA (0.05%) was used as the positive control for PCR. (D) Semiquantitative analysis of the ChIP data was performed by determining the density of each PCR band, using Quantity One (Bio-Rad). The resulting value for each ChIP sample was then plotted relative to the value of the input signal to reflect the degree of enrichment of each histone modification or protein. Three independent biological replicates were performed to generate standard deviations.

differentiating K562 cells (Fig. 5C). Quantitative analysis confirmed these observations and also revealed decreased monomethylated H3K9 at the *RUNX1* promoter; this change was not apparent by visualization (Fig. 5D). These findings demonstrate that the reductions of monomethylated H4K20 and L3MBTL1 at the *RUNX1* promoter are an early event in megakaryopoiesis.

Catalytically active PR-Set7 is required to prevent megakaryopoiesis. It was previously reported that the expression of RUNX1 sensitizes K562 cells to megakaryocytic differentiation upon TPA treatment (7). Therefore, our findings predicted that the depletion of monomethylated H4K20 and the associated activation of RUNX1 would have a similar sensitizing effect. To test this hypothesis, K562 cells were first cotransfected with a plasmid that constitutively expresses GFP and either a FLAG-tagged RUNX1 plasmid or an empty FLAG-null plasmid as the negative control prior to treatment with TPA. FACS analysis was performed with these different cells at 5 days posttransfection to determine the number of CD41-positive cells within the GFP-positive cell population (see Fig. S4 in the supplemental material). Consistent with the previous report, we observed an ~50% increase in the number of CD41-positive cells in the FLAG-RUNX1 TPA-treated cells compared to the levels in the control (see Fig. S5 in the supplemental material). Similar experiments were performed using the FLAG-null plasmid or the FLAG-PR-Set7 CD plasmid that acts as a dominant negative by depleting cells of monomethylated H4K20 without reducing levels of PR-Set7. Similar to the results in HeLa cells, Western analysis confirmed the specific decrease of monomethylated H4K20 and increased RUNX1 in the FLAG-PR-Set7 CD cells compared to the levels in the control cells (Fig. 6A). These cells were treated with a vehicle control or increasing amounts of TPA, and FACS analysis was performed as described above. As predicted, we observed a dose-dependent increase in the number of CD41 positive cells in the FLAG-null cells with increasing amounts of TPA (Fig. 6B). In contrast, the FLAG-PR-Set7 CD cells displayed a >50% increase in the number of CD41 positive cells compared to the levels in the FLAG-null control cells when treated with only the vehicle. Importantly, the number of CD41-positive cells did not increase with increasing amounts of TPA in the FLAG-PR-Set7 CD cells, strongly suggesting that they had already achieved the maximal differentiation potential. Collectively, these findings indicate that the absence of catalytically active PR-Set7 and monomethylated H4K20 results in the spontaneous megakaryocytic differentiation of K562 cells.

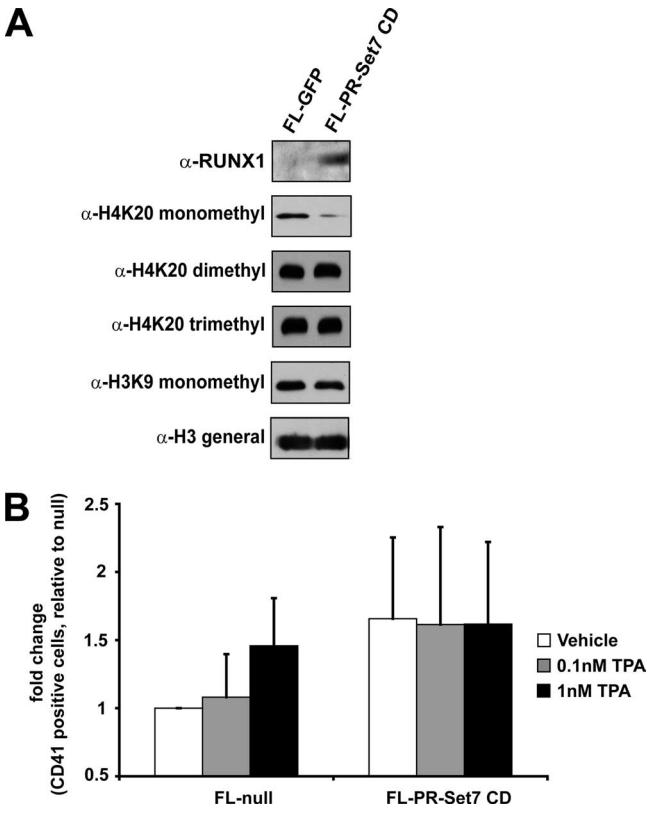

FIG. 6. Depletion of monomethylated H4K20 induces spontaneous megakaryopoiesis. (A) K562 cells were cotransfected with a plasmid expressing GFP and either a FLAG-null plasmid (control) or the FLAG-PR-Set7 R265G CD mutant that depletes cells of monomethylated H4K20. Western blot analysis was performed on these cells with the indicated antibodies. A general H3 antibody (α-H3) was used as a loading control. FL, FLAG. (B) FACS analysis was performed on these cells, treated with increasing amounts of TPA, to determine the number of CD41-positive cells within the population of GFP-positive cells. The results were plotted as increases relative to the levels in the vehicle-treated FLAG-null cells (*y* axis). Four biological replicates for each sample were performed to generate standard deviations.

DISCUSSION

In this study, we expand on our previous observations regarding a novel mammalian *trans*-tail histone code involving the monomethylation of histones H4K20 and H3K9 (36). A similar *trans*-tail histone code, where H4K20 trimethylation by the Suv4-20 enzymes was dependent upon the prior trimethylation of H3K9 by Su(var)3-9, was recently identified in *Drosophila* pericentric heterochromatin (35). While we predicted a similar temporal pathway for the monomethylated *trans*-tail histone code, surprisingly we discovered the opposite, that global H3K9 monomethylation was dependent upon the presence of the PR-Set7 H4K20 monomethyltransferase but independent of the catalytic function of PR-Set7. Since we previously described that the monomethylations of these two histone residues are enriched at the same genomic regions, including the *RUNX1* promoter, these new findings predict that an unidentified H3K9 monomethyltransferase is targeted to these regions by interacting with PR-Set7. The obvious candidates for this interaction are G9a and GLP1 (38, 39); however, we have so far not been able to detect binding of these proteins to PR-Set7 (see Fig. S6 in the supplemental material). Other known H3K9 methyltransferases are currently being assessed for PR-Set7 binding. Since PR-Set7 likely interacts with an H3K9 methyltransferase, it was unexpected that an ~10-fold excess of wild-type or CD PR-Set7 compared to endogenous PR-Set7 (data not shown) did not result in visible increases in global levels of monomethylated H3K9. While there are several possible explanations for these observations, they cannot be properly tested until the H3K9 monomethyltransferase has been identified. Besides interacting with an H3K9 methyltransferase, an alternate possibility is that PR-Set7 interacts with an unknown H3K9 di-/tridemethylase to achieve monomethylated H3K9 both on a global scale and at target loci. Both possibilities are currently under investigation.

We report here, for the first time, that monomethylated H4K20, monomethylated H3K9, and the L3MBTL1 repressor protein converge at specific genomic regions in vivo and that they function cooperatively to repress transcription. Our findings strongly suggest that the interaction between monomethylated H4K20 and L3MBTL1 is essential for the observed repressive effect as the depletion of either results in the derepression of *RUNX1* in different cell lines. It is possible that L3MBTL1 is recruited to these regions by an interaction with PR-Set7; however, we have been unable to detect such an interaction by coimmunoprecipitation (see Fig. S6 in the supplemental material). While the expression of myc-PR-Set7 led to an increase in PR-Set7 at the *RUNX1* promoter, we consistently detected decreases in both monomethylated H4K20 and L3MBTL1 at this region, further suggesting that PR-Set7 and L3MBTL1 do not interact in vivo. The residual presence of L3MBTL1 in these experiments could be due to the persistence of low levels of monomethylated H4K20 at the *RUNX1* promoter. However, recent in vitro binding studies indicate that the MBT repeats of L3MBTL1 can also bind monomethylated H3K9, and since monomethylated H3K9 remains present at the *RUNX1* promoter in these experiments, these observations suggest that this modification may play a role in recruiting or stabilizing L3MBTL1 to this region (18). Consistent with this, in the PR-Set7 CD HeLa cells, where monomethylated H4K20 is dramatically reduced, we observed residual enrichment of monomethylated H3K9 and L3MBTL1 at the *RUNX1* promoter, again suggesting a possible in vivo interaction between them. However, the continued presence of monomethylated H3K9 at the *RUNX1* promoter was not sufficient to repress *RUNX1* transcription, suggesting that this modification does not play a direct role in gene repression. It is possible that monomethylated H3K9 and the unidentified methyltransferase are important in other aspects of this pathway, but this will remain unclear until the methyltransferase is discovered. These findings also indirectly reinforce that the interaction between monomethylated H4K20 and L3MBTL1 appears to be the critical step for repression.

PR-Set7 and monomethylated H4K20 were originally identified as being associated with repressed chromatin, and our findings here and those of another study indicate that PR-Set7 and monomethylated H4K20 clearly participate in a gene repression pathway by recruiting and binding the L3MBTL1 repressor protein in vivo (8, 25, 44). However, several recent reports document an association of monomethylated H4K20

with actively transcribed genes (2, 40, 46). One possible explanation for these apparent differences is that this histone modification could participate in both transcriptional activation and repression pathways, depending on the specific gene, similar to what has been observed for di- and trimethylated H3K9 (45). This could be achieved by the recruitment of distinct H4K20 monomethyl-binding regulatory proteins that could activate or repress transcription (30). However, a more likely possibility is that the underlying function of this pathway is to fine-tune the dosage of the corresponding gene rather than completely ablating its transcription. This theory is consistent with both observations: that monomethylated H4K20 is found within several active genes and that the depletion of this modification consistently results in the increased expression of these genes (data not shown). Further studies are required to validate this hypothesis.

RUNX1 is an important transcription factor that controls the expression of a variety of lineage-specific genes and, therefore, itself must be tightly regulated to prevent premature differentiation (12). In this report, we demonstrated that in the multipotent K562 cells the newly described repressive *trans*-tail histone code operates at *RUNX1* to control its expression and, therefore, megakaryocytic differentiation. We discovered that the loss of PR-Set7 and monomethylated H4K20 was an early event in differentiation, occurring prior to DNA ploidy and cell morphology changes, indicating that this repressive pathway participates in regulating megakaryopoiesis. Contrary to our earlier observations, global levels of monomethylated H3K9 were retained in the TPA-treated K562 cells despite the overall reduction of PR-Set7, although monomethylated H3K9 was reduced at the *RUNX1* promoter. It is interesting to note that hemin-treated cells also displayed reduced levels of PR-Set7 but retained both monomethylated H4K20 and H3K9. Taken together, these observations imply that these histone modifications are relatively stable in the two separate differentiation pathways, even in the absence of PR-Set7, with the exception of monomethylated H4K20 in the TPA-treated cells. They also imply that specific reduction of monomethylated H4K20 during megakaryopoiesis is a defining mechanistic feature of this pathway compared to erythropoiesis. It remains unclear how the selective reduction of this histone modification is achieved, although it is tempting to speculate that there is an unknown H4K20 demethylase that operates specifically in the precursor cells to initiate megakaryocytic differentiation, in part, by activating RUNX1. We demonstrated that the ectopic expression of RUNX1 sensitized K562 cells to the differentiation effects of TPA but itself was not sufficient to induce megakaryopoiesis (see Fig. S5 in the supplemental material). Surprisingly, in cells lacking monomethylated H4K20, TPA was not required to induce megakaryopoiesis; the cells tended to spontaneously differentiate. While RUNX1 is likely to be an important component of this effect, we hypothesize that other unidentified genes that contribute to megakaryopoiesis are also regulated by this repressive pathway and that the lack of monomethylated H4K20 results in their activation, culminating in megakaryocytic differentiation. It is important to note that the differentiation-associated changes in monomethylated H4K20 are not restricted to hematopoiesis. A previous report demonstrated that global levels of monomethylated H4K20 were highest in mouse neuroblasts and myoblasts and that these levels were significantly reduced during their differentiation, similar to what we observed during megakaryopoiesis (4). Collectively, these findings strongly suggest that this repressive pathway plays a fundamental role in developmental programs by preserving a multipotent phenotype via repression of certain lineage-specific genes. Consistent with this theory, a recent study demonstrated that homozygous PR-Set7 knockout mice were embryonic lethal, suggesting a role for PR-Set7 and monomethylated H4K20 in mammalian embryogenesis (11). Similarly, *Drosophila* organisms lacking PR-Set7 fail to progress past the third instar, again demonstrating a critical role for PR-Set7 and monomethylated H4K20 in development (8, 25). The identification of the genes regulated by this repressive pathway will provide critical insights into the complex biological problem of development and differentiation.

ACKNOWLEDGMENTS

We thank Adam Goldfarb for the K562 cell line, Danny Reinberg for the PR-Set7 antibody, Yochi Shinkai for the G9a MEFs and plasmids, Tanya Spektor for the PR-Set7-PCNA binding control data, Michael Stallcup for critical review of the manuscript, and the entire Rice laboratory for helpful thoughts and discussions.

This work was supported by a grant from the Pew Charitable Trusts and from the NIH to J.C.R. (GM075094). J.K.S. was partially supported by a predoctoral traineeship from the NIH (T32 GM067587).

REFERENCES

1. **Allis, C. D., S. L. Berger, J. Cote, S. Dent, T. Jenuwien, T. Kouzarides, L. Pillus, D. Reinberg, Y. Shi, R. Shiekhattar, A. Shilatifard, J. Workman, and Y. Zhang.** 2007. New nomenclature for chromatin-modifying enzymes. Cell **131:**633–636.
2. **Barski, A., S. Cuddapah, K. Cui, T. Y. Roh, D. E. Schones, Z. Wang, G. Wei, I. Chepelev, and K. Zhao.** 2007. High-resolution profiling of histone methylations in the human genome. Cell **129:**823–837.
3. **Bernstein, B. E., A. Meissner, and E. S. Lander.** 2007. The mammalian epigenome. Cell **128:**669–681.
4. **Biron, V. L., K. J. McManus, N. Hu, M. J. Hendzel, and D. A. Underhill.** 2004. Distinct dynamics and distribution of histone methyl-lysine derivatives in mouse development. Dev. Biol. **276:**337–351.
5. **Cao, R., L. Wang, H. Wang, L. Xia, H. Erdjument-Bromage, P. Tempst, R. S. Jones, and Y. Zhang.** 2002. Role of histone H3 lysine 27 methylation in Polycomb-group silencing. Science **298:**1039–1043.
6. **Couture, J. F., E. Collazo, J. S. Brunzelle, and R. C. Trievel.** 2005. Structural and functional analysis of SET8, a histone H4 Lys-20 methyltransferase. Genes Dev. **19:**1455–1465.
7. **Elagib, K. E., F. K. Racke, M. Mogass, R. Khetawat, L. L. Delehanty, and A. N. Goldfarb.** 2003. RUNX1 and GATA-1 coexpression and cooperation in megakaryocytic differentiation. Blood **101:**4333–4341.
8. **Fang, J., Q. Feng, C. S. Ketel, H. Wang, R. Cao, L. Xia, H. Erdjument-Bromage, P. Tempst, J. A. Simon, and Y. Zhang.** 2002. Purification and functional characterization of SET8, a nucleosomal histone H4-lysine 20-specific methyltransferase. Curr. Biol. **12:**1086–1099.
9. **Fischle, W., Y. Wang, S. A. Jacobs, Y. Kim, C. D. Allis, and S. Khorasanizadeh.** 2003. Molecular basis for the discrimination of repressive methyl-lysine marks in histone H3 by Polycomb and HP1 chromodomains. Genes Dev. **17:**1870–1881.
10. **Gopalakrishnan, T. V., and W. F. Anderson.** 1979. Mouse erythroleukemia cells. Methods Enzymol. **58:**506–511.
11. **Huen, M. S., S. M. Sy, J. M. van Deursen, and J. Chen.** 2008. Direct interaction between SET8 and proliferating cell nuclear antigen couples H4-K20 methylation with DNA replication. J. Biol. Chem. **283:**11073–11077.
12. **Ichikawa, M., T. Asai, S. Chiba, M. Kurokawa, and S. Ogawa.** 2004. Runx1/AML-1 ranks as a master regulator of adult hematopoiesis. Cell Cycle **3:**722–724.
13. **Ichikawa, M., T. Asai, T. Saito, S. Seo, I. Yamazaki, T. Yamagata, K. Mitani, S. Chiba, S. Ogawa, M. Kurokawa, and H. Hirai.** 2004. AML-1 is required for megakaryocytic maturation and lymphocytic differentiation, but not for maintenance of hematopoietic stem cells in adult hematopoiesis. Nat. Med. **10:**299–304.
14. **Julien, E., and W. Herr.** 2004. A switch in mitotic histone H4 lysine 20 methylation status is linked to M phase defects upon loss of HCF-1. Mol. Cell **14:**713–725.
15. **Kim, J., J. Daniel, A. Espejo, A. Lake, M. Krishna, L. Xia, Y. Zhang, and M. T. Bedford.** 2006. Tudor, MBT and chromo domains gauge the degree of lysine methylation. EMBO Rep. **7:**397–403.

16. **Kurokawa, M.** 2006. AML1/Runx1 as a versatile regulator of hematopoiesis: regulation of its function and a role in adult hematopoiesis. Int. J. Hematol. **84:**136–142.
17. **Kuzmichev, A., K. Nishioka, H. Erdjument-Bromage, P. Tempst, and D. Reinberg.** 2002. Histone methyltransferase activity associated with a human multiprotein complex containing the Enhancer of Zeste protein. Genes Dev. **16:**2893–2905.
18. **Li, H., W. Fischle, W. Wang, E. M. Duncan, L. Liang, S. Murakami-Ishibe, C. D. Allis, and D. J. Patel.** 2007. Structural basis for lower lysine methylation state-specific readout by MBT repeats of L3MBTL1 and an engineered PHD finger. Mol. Cell **28:**677–691.
19. **Luger, K., A. W. Mader, R. K. Richmond, D. F. Sargent, and T. J. Richmond.** 1997. Crystal structure of the nucleosome core particle at 2.8 A resolution. Nature **389:**251–260.
20. **Mikkelsen, T. S., M. Ku, D. B. Jaffe, B. Issac, E. Lieberman, G. Giannoukos, P. Alvarez, W. Brockman, T. K. Kim, R. P. Koche, W. Lee, E. Mendenhall, A. O'Donovan, A. Presser, C. Russ, X. Xie, A. Meissner, M. Wernig, R. Jaenisch, C. Nusbaum, E. S. Lander, and B. E. Bernstein.** 2007. Genome-wide maps of chromatin state in pluripotent and lineage-committed cells. Nature **448:**553–560.
21. **Min, J., A. Allali-Hassani, N. Nady, C. Qi, H. Ouyang, Y. Liu, F. MacKenzie, M. Vedadi, and C. H. Arrowsmith.** 2007. L3MBTL1 recognition of mono- and dimethylated histones. Nat. Struct. Mol. Biol. **14:**1229–1230.
22. **Min, J., Y. Zhang, and R. M. Xu.** 2003. Structural basis for specific binding of Polycomb chromodomain to histone H3 methylated at Lys 27. Genes Dev. **17:**1823–1828.
23. **Muller, J., C. M. Hart, N. J. Francis, M. L. Vargas, A. Sengupta, B. Wild, E. L. Miller, M. B. O'Connor, R. E. Kingston, and J. A. Simon.** 2002. Histone methyltransferase activity of a Drosophila Polycomb group repressor complex. Cell **111:**197–208.
24. **Nelson, J. D., O. Denisenko, P. Sova, and K. Bomsztyk.** 2006. Fast chromatin immunoprecipitation assay. Nucleic Acids Res. **34:**e2.
25. **Nishioka, K., J. C. Rice, K. Sarma, H. Erdjument-Bromage, J. Werner, Y. Wang, S. Chuikov, P. Valenzuela, P. Tempst, R. Steward, J. T. Lis, C. D. Allis, and D. Reinberg.** 2002. PR-Set7 is a nucleosome-specific methyltransferase that modifies lysine 20 of histone H4 and is associated with silent chromatin. Mol. Cell **9:**1201–1213.
26. **North, T. E., T. Stacy, C. J. Matheny, N. A. Speck, and M. F. de Bruijn.** 2004. Runx1 is expressed in adult mouse hematopoietic stem cells and differentiating myeloid and lymphoid cells, but not in maturing erythroid cells. Stem Cells **22:**158–168.
27. **Okuda, T., J. van Deursen, S. W. Hiebert, G. Grosveld, and J. R. Downing.** 1996. AML1, the target of multiple chromosomal translocations in human leukemia, is essential for normal fetal liver hematopoiesis. Cell **84:**321–330.
28. **Papp, B., and J. Muller.** 2006. Histone trimethylation and the maintenance of transcriptional ON and OFF states by trxG and PcG proteins. Genes Dev. **20:**2041–2054.
29. **Peterson, C. L., and M. A. Laniel.** 2004. Histones and histone modifications. Curr. Biol. **14:**R546–R551.
30. **Rice, J. C., and C. D. Allis.** 2001. Histone methylation versus histone acetylation: new insights into epigenetic regulation. Curr. Opin. Cell Biol. **13:** 263–273.
31. **Rice, J. C., S. D. Briggs, B. Ueberheide, C. M. Barber, J. Shabanowitz, D. F. Hunt, Y. Shinkai, and C. D. Allis.** 2003. Histone methyltransferases direct different degrees of methylation to define distinct chromatin domains. Mol. Cell **12:**1591–1598.
32. **Rice, J. C., K. Nishioka, K. Sarma, R. Steward, D. Reinberg, and C. D. Allis.** 2002. Mitotic-specific methylation of histone H4 Lys 20 follows increased PR-Set7 expression and its localization to mitotic chromosomes. Genes Dev. **16:**2225–2230.
33. **Rice, K. L., I. Hormaeche, and J. D. Licht.** 2007. Epigenetic regulation of normal and malignant hematopoiesis. Oncogene **26:**6697–6714.
34. **Rutherford, T. R., J. B. Clegg, and D. J. Weatherall.** 1979. K562 human leukaemic cells synthesise embryonic haemoglobin in response to haemin. Nature **280:**164–165.
35. **Schotta, G., M. Lachner, K. Sarma, A. Ebert, R. Sengupta, G. Reuter, D. Reinberg, and T. Jenuwein.** 2004. A silencing pathway to induce H3-K9 and H4-K20 trimethylation at constitutive heterochromatin. Genes Dev. **18:**1251–1262.
36. **Sims, J. K., S. I. Houston, T. Magazinnik, and J. C. Rice.** 2006. A trans-tail histone code defined by monomethylated H4 Lys-20 and H3 Lys-9 demarcates distinct regions of silent chromatin. J. Biol. Chem. **281:**12760–12766.
37. **Strahl, B. D., and C. D. Allis.** 2000. The language of covalent histone modifications. Nature **403:**41–45.
38. **Tachibana, M., K. Sugimoto, M. Nozaki, J. Ueda, T. Ohta, M. Ohki, M. Fukuda, N. Takeda, H. Niida, H. Kato, and Y. Shinkai.** 2002. G9a histone methyltransferase plays a dominant role in euchromatic histone H3 lysine 9 methylation and is essential for early embryogenesis. Genes Dev. **16:**1779–1791.
39. **Tachibana, M., J. Ueda, M. Fukuda, N. Takeda, T. Ohta, H. Iwanari, T. Sakihama, T. Kodama, T. Hamakubo, and Y. Shinkai.** 2005. Histone methyltransferases G9a and GLP form heteromeric complexes and are both crucial for methylation of euchromatin at H3-K9. Genes Dev. **19:**815–826.
40. **Talasz, H., H. H. Lindner, B. Sarg, and W. Helliger.** 2005. Histone H4-lysine 20 monomethylation is increased in promoter and coding regions of active genes and correlates with hyperacetylation. J. Biol. Chem. **280:**38814–38822.
41. **Tani, T., J. Ylanne, and I. Virtanen.** 1996. Expression of megakaryocytic and erythroid properties in human leukemic cells. Exp. Hematol. **24:**158–168.
42. **Taverna, S. D., H. Li, A. J. Ruthenburg, C. D. Allis, and D. J. Patel.** 2007. How chromatin-binding modules interpret histone modifications: lessons from professional pocket pickers. Nat. Struct. Mol. Biol. **14:**1025–1040.
43. **Tetteroo, P. A., F. Massaro, A. Mulder, R. Schreuder-van Gelder, and A. E. von dem Borne.** 1984. Megakaryoblastic differentiation of proerythroblastic K562 cell-line cells. Leuk. Res. **8:**197–206.
44. **Trojer, P., G. Li, R. J. Sims III, A. Vaquero, N. Kalakonda, P. Boccuni, D. Lee, H. Erdjument-Bromage, P. Tempst, S. D. Nimer, Y. H. Wang, and D. Reinberg.** 2007. L3MBTL1, a histone-methylation-dependent chromatin lock. Cell **129:**915–928.
45. **Vakoc, C. R., S. A. Mandat, B. A. Olenchock, and G. A. Blobel.** 2005. Histone H3 lysine 9 methylation and HP1gamma are associated with transcription elongation through mammalian chromatin. Mol. Cell **19:**381–391.
46. **Vakoc, C. R., M. M. Sachdeva, H. Wang, and G. A. Blobel.** 2006. Profile of histone lysine methylation across transcribed mammalian chromatin. Mol. Cell. Biol. **26:**9185–9195.
47. **Wanda, P. E., L. T. Lee, and C. Howe.** 1981. A spectrophotometric method for measuring hemoglobin in erythroleukemic cells (K562). J. Histochem. Cytochem. **29:**1442–1444.
48. **Wu, R., A. V. Terry, P. B. Singh, and D. M. Gilbert.** 2005. Differential subnuclear localization and replication timing of histone H3 lysine 9 methylation states. Mol. Biol. Cell **16:**2872–2881.
49. **Wu, S., R. C. Trievel, and J. C. Rice.** 2007. Human SFMBT is a transcriptional repressor protein that selectively binds the N-terminal tail of histone H3. FEBS Lett. **581:**3289–3296.
50. **Xiao, B., C. Jing, G. Kelly, P. A. Walker, F. W. Muskett, T. A. Frenkiel, S. R. Martin, K. Sarma, D. Reinberg, S. J. Gamblin, and J. R. Wilson.** 2005. Specificity and mechanism of the histone methyltransferase Pr-Set7. Genes Dev. **19:**1444–1454.